

Ambient temperature growth of mono- and polycrystalline NbN nanofilms and their surface and composition analysis

TRANSACTIONS ON APPLIED SUPERCONDUCTIVITY

S. Krause, V. Afanas'ev, V. Desmaris, D. Meledin, A. Pavolotsky, V. Belitsky, A. Lubenschenko, A. Batrakov, M. Rudziński, E. Pippel

Abstract—This paper presents the studies of high-quality 5 nm thin NbN films deposited by means of reactive DC magnetron sputtering at room temperature. The deposition without substrate heating offers major advantages from a processing point of view and motivates the extensive composition- and surface characterization and comparison of the present films with high quality films grown at elevated temperatures. Monocrystalline NbN films have been epitaxially grown onto hexagonal GaN buffer-layers (0002) and show a distinct, low defect interface as confirmed by High-Resolution TEM. The critical temperature T_c of films on the GaN buffer-layer reached 10.4 K. Furthermore, a poly-crystalline structure was observed on films grown onto Si (100) substrates, exhibiting a T_c of 8.1 K albeit a narrow transition from the normal to the superconducting state. X-ray photoelectron spectroscopy and reflected electron energy loss spectroscopy verified that the composition of NbN was identical irrespectively of applied substrate heating. Moreover, the native oxide layer at the surface of NbN has been identified as NbO₂ and thus, is in contrast to the Nb₂O₅, usually claimed to be formed at the surface of Nb when exposed to air. These findings are of significance since it was proven the possibility of growing epitaxial NbN onto GaN buffer layer in the absence of high temperatures hence paving the way to employ NbN in more advanced fabrication processes involving a higher degree of complexity. The eased integration and employment of lift-off techniques could, in particular, lead to improved performance of cryogenic ultra-sensitive terahertz electronics.

Index Terms—Epitaxy, NbN, ultra-thin film, GaN, sputtering

I. INTRODUCTION

Niobium-nitride with its relatively high energy bandgap of 2.5 meV has always had the attraction to be employed in Terahertz applications. In particular, ultra-thin NbN material

was firstly employed in heterodyne low-noise receivers in 1990 with the development of the phonon-cooled hot electron bolometer HEB [1] and yet this material is attracting rising attention in recent submillimeter and THz receiver research [2,3]. NbN exhibits short intrinsic electron-electron and electron-phonon interaction times, thus favoring its application in HEB where it yields intermediate frequency (IF) bandwidth of typically 4 GHz [4-6] and is considered superior over niobium-based SIS junctions in terms of LO consumption and sensitivity above 1.3 THz.

The performance of HEB's is ultimately limited by the quality, e.g. critical temperature, transition sharpness and uniformity of the 3-6 nm thin NbN layer [7,8]. The suppression of superconductivity for films with thicknesses close to their coherence length is considered a major challenge. Poly-crystalline, yet high quality, ultra-thin NbN films on commonly used substrates such as Si only exhibit T_c of approximately 9 K [9]. This has led to the employment of lattice-matched buffer-layers such as MgO [10], 3C-SiC [11,12] and the recently reported hexagonal GaN [13], which have proven to dramatically improve the superconducting properties, particularly for ultra-thin films [14]. Additionally, introducing strain to the NbN film through a buffer-layer such as Nb₅N₆ also showed to improve its properties [15]. The growth in a reactive argon/nitrogen atmosphere by means of DC magnetron sputtering usually requires high temperatures, achieved by heating the substrate to up to 950 °C in order to obtain the desired cubic δ -phase of NbN with T_c of the bulk material of 16 K. The presence of a high temperature environment limits the overall complexity of the device remarkably and precludes for instance the integration of other circuitries containing thin insulating layers or intricate multi-layer structures. Moreover, lift-off techniques used for patterning are also not compatible with a high temperature process.

In this paper we demonstrate the possibility of growing epitaxial NbN onto GaN buffer-layers without substrate heating and thus confirming and extending the applicability of GaN (0002) as lattice-matched substrate for NbN in its (111) orientation. The wurtzite-GaN layer was of approximately 2 μ m thickness and grown onto a 2-inch sapphire (0001) substrate by means of metal-organic chemical vapor

S. Krause, V. Desmaris, D. Meledin, A. Pavolotsky and V. Belitsky are with the Group for Advanced Receiver Development (GARD) at the Chalmers University of Technology, Gothenburg, Sweden (e-mail: sascha.krause@chalmers.se).

V. Afanas'ev, A. Lubenschenko and A. Batrakov are with the Department of General Physics and Nuclear Fusion, National Research University "Moscow Power Engineering Institute", Moscow, Russia.

M. Rudziński is with the Institute of Electronic Materials Technology (ITME), Warsaw, Poland.

E. Pippel is with the Max Planck Institute of Microstructure Physics, Halle/Saale, Germany.

deposition (MOCVD). Furthermore, the careful adjustment of deposition conditions also enabled the growth of polycrystalline, yet high quality ultra-thin films on bare Si substrates at ambient temperatures. X-ray photoelectron spectroscopy (XPS) as a highly sensitive surface characterization techniques and reflected electron energy loss spectroscopy (REELS) [16] revealed the composition of the NbN films and their native oxides which are formed at the surface when exposed to air. Up to now, only minor research has been done on the investigation of the oxide state of NbN surfaces [17-20], in particular on ultra-thin films, although it has a great impact on applied cleaning procedures and therefore the quality of the contact to the NbN layer.

II. EXPERIMENT

A. Substrate preparation and deposition parameters

The 2 μm thick GaN buffer-layer (0002) was prepared at the Institute of Electronic Materials Technology (ITME), Warsaw, and grown onto a sapphire template by a MOCVD process using an RF heated AIX200/4RF-S low pressure horizontal reactor. The Si-substrates are of (100)-orientation and exhibited a native oxide layer of approximately 2 nm thickness, which was not removed. Substrate surfaces were ultra-sonically cleaned in acetone and isopropanol before loading and in-situ exposed to an argon plasma prior to the actual sputter process.

The DC sputter tool used was an AJA Orion-6UD with 2-inch high-purity Nb (99.95%) target. The argon and reactive nitrogen content was fine-tuned and kept constant at a ratio of 1:9.2. Consequently, the deposition rate amounted to 1.2 $\text{\AA}/\text{s}$ confirmed by HRTEM characterization. The substrate holder was not heated and remained at ambient temperature throughout the entire deposition process. Additionally, the deposition of NbN with 5 nm and 10 nm thickness onto bare Si-substrates at temperatures of 650 $^{\circ}\text{C}$ served as a reference for subsequent comparison of the composition and surface state.

B. Characterization techniques / analysis

The superconducting properties such as critical temperature T_c , resistivity ρ and transition sharpness ΔT were obtained with a dipstick which was slowly lowered into a liquid helium Dewar while recording the temperature and film resistance.

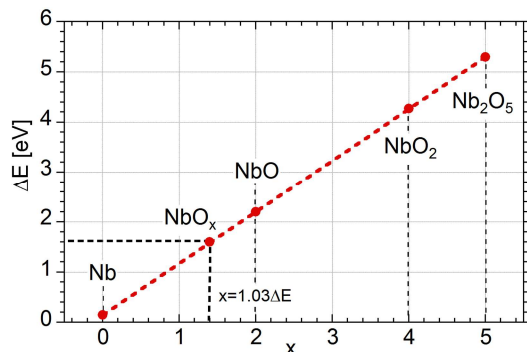


Fig. 1. Energy difference in binding energies for NbO_x compounds. [20]

All films have been exposed to ambient air for approximately 1 month until they were examined by X-ray Photoelectron Spectroscopy and Reflected Electron Energy Loss Spectroscopy. The Kimball Physics EMG 4212 tool with BaO cathodes was used as source for the primary electrons and the SPECS XR-50 for the generation of X-rays. Electron energy spectra were recorded by the semispherical energy analyzer SPECS Phoibos 225 with absolute energy resolution of 0.3 eV within 0-15 keV range and subsequently superimposed by the bonding-peaks of Nb 3p $_{3/2}$, Nb-O and Nb-N. The nature of the present oxide was identified by looking at the energy shift ΔE relative to Nb, according to Fig. 1. Moreover, not only the oxides have been investigated following this method, also the energy peak of the Nb-N bond reveals eventual differences in film composition upon different growth conditions.

Furthermore, the samples were prepared for HRTEM by depositing a thin Nb, respectively Ti/Au layer onto the NbN nanofilms in order to increase the contrast.

III. RESULTS AND DISCUSSION

A. Superconducting properties

High critical temperature as well as a sharp transition from

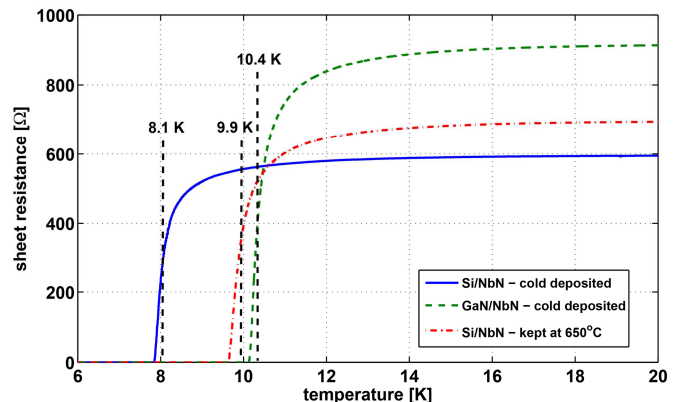


Fig. 2. Film's sheet resistance as a function of bath temperature for NbN grown on Si and GaN buffer-layer for heated and cold substrates.

the normal to the superconducting state are indicators of high quality growth and desired features for particularly HEB's. Those parameters can easily be extracted from the resistance versus temperature curves. The Fig. 2 is an excerpt of the resistance response in the temperature range from 6 K to 20 K, thus emphasizing the transition from the normal to the superconducting state. The critical temperature is defined as the drop of resistance to 50 % of its normal state value, usually taken at 20 K. The red trace shows the NbN film grown onto Si substrates utilizing substrate heating at 650 $^{\circ}\text{C}$. The transition is within 1.7 K and T_c amounts to 9.9 K. In comparison the film deposited at ambient substrate temperature exhibits a transition width of 1.4 K although lower T_c of 8.1 K. In contrast to the films deposited onto hot substrates, its normal state resistance is lowered by approximately 14 %. This can already be seen as significant improvement over earlier-reported cold-deposited NbN film

on Si substrates with T_c of 5 K [21]. The NbN film grown onto the GaN buffer-layer is depicted by the green curve and shows also a narrow transition width of 1.5 K and increased T_c compared to the silicon samples, reaching 10.4 K.

B. Composition and surface analysis

Structural features and layer-thickness of the NbN nanofilms were revealed by employing HRTEM analysis. In Fig. 3, it can be seen that the NbN nanofilm grew epitaxially onto the GaN buffer-layer, despite the ambient substrate temperature. The interface is distinct and only very few defects are present. The thickness of the obtained NbN layer

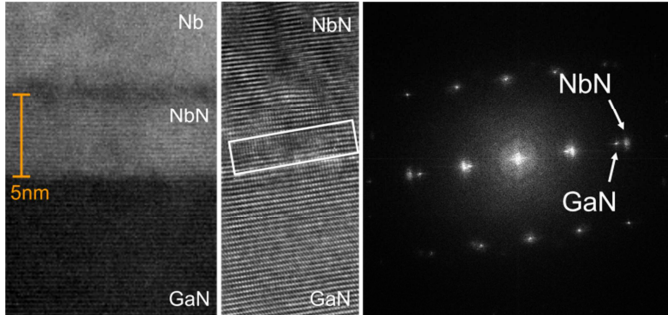


Fig. 3. HRTEM image of cross-section of the NbN/GaN compound and magnified interface. The superimposed diffraction pattern of NbN and GaN reveals a mono-crystalline structure and coincide almost perfectly.

amounts to 5 nm with insignificant deviation across the film area, hence confirming the expected deposition rate. Furthermore, the diffraction pattern has been generated from Fast Fourier Transformation of selected areas inside the film and compared to those taken from the inside of the GaN layer. The distinguished spots reveal a monocrystalline structure of both the NbN and GaN layer and the proper alignment gives evidence of the epitaxial growth and lattice match.

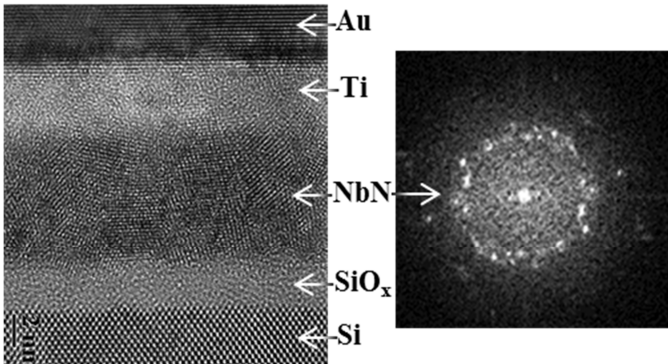


Fig. 4. HRTEM image of NbN grown onto the Si substrate with amorphous native oxide of 2 nm thickness shows small differently oriented grains. The diffraction pattern is typical for a poly-crystalline growth.

In contrast, a polycrystalline structure was identified for the NbN films grown onto Si substrates as illustrated in Fig. 4. Moreover, the formation of small differently oriented grains can be seen. The interface of the Si substrate and NbN consist of approximately 2 nm native amorphous silicon oxide SiO_x .

The diffraction pattern in this case does not feature particular spots as typical for the mono-crystalline growth. The smeared and circular pattern is accompanied with the

poly-crystalline film growth and can be seen as a superposition of diffraction pattern of the differently oriented grains.

XPS is considered a sensitive surface characterization technique due to the low escape depth of electrons and is employed to identify the type of the native oxide at the NbN

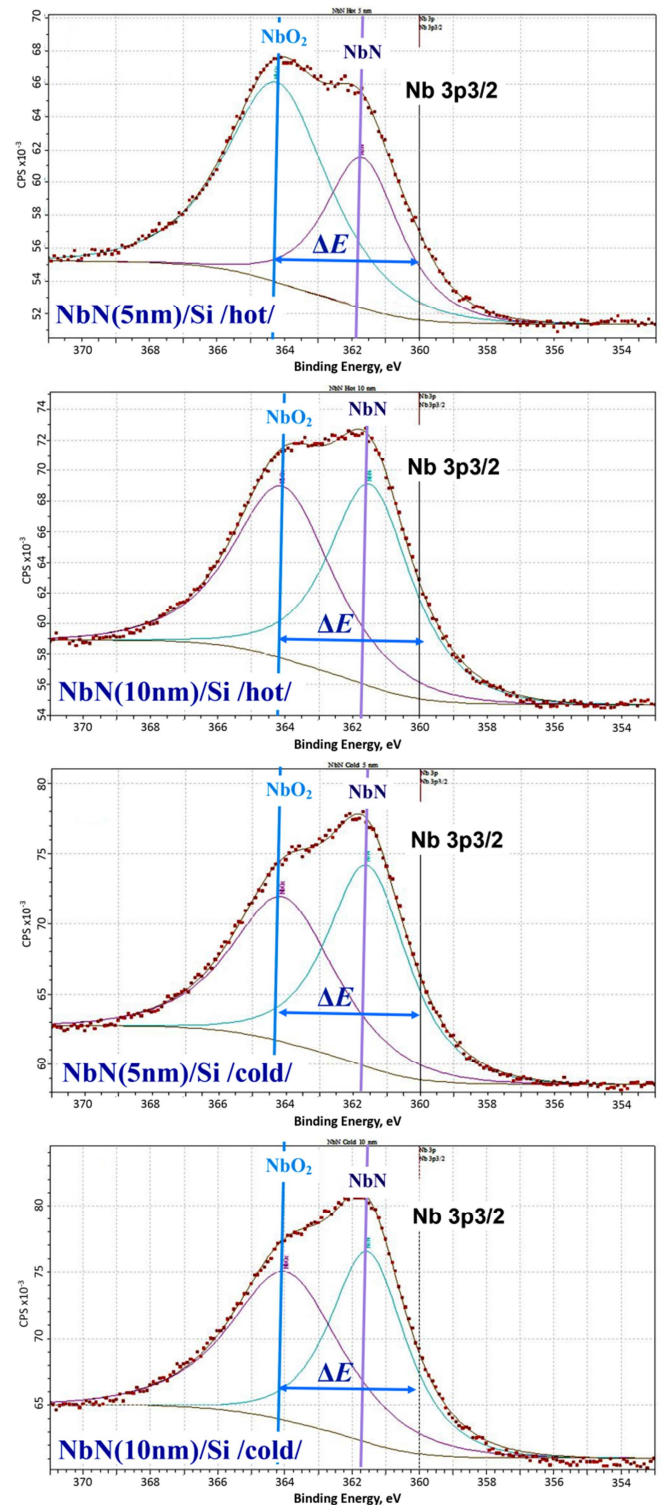


Fig. 5. XPS spectra of the investigated NbN films. The dots represent measurement data and the solid lines superimposed peaks of Nb 3p3/2, Nb-O and NbN bonds.

film surface. The following energy spectra were taken from NbN/Si films of respectively 5 nm and 10 nm thickness, grown at 650°C substrate temperature and in the absence of substrate heating.

The recorded spectra were superimposed by the peaks of Nb 3p3/2, Nb-O and Nb-N bonds. Fig. 5 depicts that the Nb 3p3/2 bond is not present in all NbN spectra and thus, confirms the absence of metallic Nb. The measured energy shift ΔE of 4.1 eV of the Nb-O bond relative to the Nb 3p3/2 peak reveals, according to Fig. 1, the formation of NbO₂ at the surface of all investigated NbN films. Furthermore, evidence of the Nb₂O₅ peak cannot be found in the recorded data. Note that the identified Nb-N bond resolves at the same binding energy of 361.75±0.07 eV, independently of film thickness and substrate temperature. The peak-intensities of the spectra according Fig. 5 are used to estimate the thicknesses of the oxide layer according to Eq. 1.

$$d_{NbO_2} = \cos(\gamma) \cdot \lambda_{inNbO_2} \cdot \ln \left(\frac{I_{NbO_2}}{I_{NbN}} \cdot \frac{\lambda_{inNbN}}{\lambda_{inNbO_2}} + 1 \right) \quad (1)$$

Where the inelastic mean free path λ_{in} of NbO₂ and NbN is calculated accordingly to [23] and the angle γ of 57.74° is between the incident X-ray beam and the energy analyzer.

Relevant data such as energy shift, oxide nature and calculated thickness is summarized in Table 1.

TABLE I

EXTRACTED OXIDE THICKNESS AND COMPOSITION OF INVESTIGATED SAMPLES

Sample	ΔE [eV]	Oxide composition	Oxide thickness [nm]
Nb	4.9	Nb ₂ O ₅	1.5
NbN 5nm cold	4.1	NbO ₂	0.9
NbN 5nm hot	4.0	NbO ₂	0.6
NbN 10nm cold	4.1	NbO ₂	0.5
NbN 10nm hot	4.1	NbO ₂	0.6

Summary of extracted energy shift, oxide composition and oxide thickness for different NbN films grown on Si substrates at ambient and elevated substrate holder temperatures.

All investigated NbN films possess the same type of native oxide with similar thicknesses between 0.5 to 0.9 nm, in contrast to the analyzed pure Nb sample with Nb₂O₅ oxide composition and slightly thicker oxide layer thickness of 1.5 nm.

These findings are also supported by the recorded REELS spectra, analyzed similarly to [24] as seen in Fig. 6, since the plasmon peaks of all NbN films are coinciding at the same position of 25.4 eV, thus verifying the identical composition. Furthermore, the plasmon oscillation peak of NbO₂ at 15.2 eV [20] is present in our NbN spectra, however, not visible in the one for Nb.

This is extending the understanding of the nature of the native oxides of NbN films, which up to now was described only for films between 600 nm to 1500 nm thickness [19] and thermal oxidation of bulk NbN material [17,18]. They identified mainly the formation of Nb₂O₅ similar to the process taking place on the surface of pure Nb as well as they observed that below temperatures of 450 °C an amorphous or poly-crystalline oxide was formed, which is in agreement with the present work.

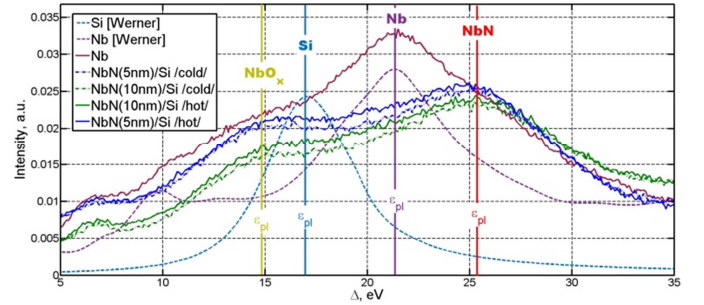


Fig. 6. Differential inverse mean free path extracted by Tougaard method [25]

IV. CONCLUSION

We have proven the possibility to epitaxially grow ultra-thin NbN onto GaN buffer-layers at ambient deposition temperatures. The critical temperature of these films reached 10.4 K and is thus higher than the T_c of films grown onto Si substrates in a high temperature environment. HRTEM revealed a seamless interface with low defect density and verified the expected thickness of 5 nm. Additionally, NbN was also grown onto bare Si substrates exhibiting T_c of 8.1 K with narrow normal-to-superconductor transition width and low sheet resistance of 590 Ohm/sq. It has been shown that the stoichiometry of all sputtered NbN films on Si substrates is identical, hence independent of growth temperature. This altogether will prospectively allow the use of NbN in more advanced fabrication processes such as lift-off and multi-layer structures. XPS and REELS revealed the type of the native oxide to be of the lower order oxide NbO₂, which is in contrast to previously observed Nb₂O₅ present on thicker films and bulk NbN. These findings have an impact on the handling practices of ultra-thin NbN films i.e. the application of appropriate cleaning procedures and surface treatment to improve for instance the contact to NbN.

REFERENCES

- [1] E. Gershenzon, G. Gol'tsman, I. Gogodze, Y. Gusev, A. Elant'ev, B. Karasik, A. Semenov, " Millimeter and submillimeter range mixer biased on electronic heating of superconducting films in the resistive state", *Sov. Phys. – Supercond.*, vol. 3, no. 10, p. 1582-1597, 1990.
- [2] D. Buchel, P. Putz, K. Jacobs, M. Schultz, M. U. Graf, H. Richter, O. Ricken, H.-W. Hubers, R. Gusten, C. Honingh, J. Stuzki, "4.7-THz superconducting hot electron bolometer waveguide mixer", *IEEE Transactions on Terahertz Science and Technology*, vol. 5, no. 2, 2015.
- [3] A. Khudchenko, A. Baryshev, K. Rudakov, V. Koshelets, P. Dmitriev, R. Hesper, L. Jong, "High gap Nb-AlN-NbN SIS junctions for frequency band 790-950 GHz", *26th International Symposium on Space Terahertz Technology*, 2015.
- [4] A. Semenov, H. Richter, H. Hübers, A. Kuzmin, K. Ilin, M. Siegel, D. Petrenko, I. Tretyakov, S. Ryabchun, M. Finkel, N. Kaurova, G. Gol'tsman, "Optimization of the intermediate frequency bandwidth in the THz HEB mixers", *24th International Symposium on Space Terahertz Technology*, 2013.
- [5] D. Meledin, A. Pavolotsky, V. Desmaris, I. Lapkin, C. Risacher, V. Perez, D. Henke, O. Nyström, E. Sundin, D. Dochev, M. Pantaleev, M. Fredrixon, M. Strandberg, B. Voronov, G. Gol'tsman och V. Belitsky, "A 1.3-THz Balanced Waveguide HEB Mixer for the APEX Telescope," *IEEE Transactions on Microwave Theory and Techniques*, vol. 57, no. 1, 2009.
- [6] I. Tretyakov, S. Ryabchun, M. Finkel, A. Maslennikova, N. Kaurova, A. Lobastova, B. Voronov, G. Gol'tsman, "Low noise and wide bandwidth of NbN hot electron bolometer mixer", *Appl. Phys. Lett.*, vol. 98, no. 3, 2011.
- [7] A. Sergeev, M. Reizer, "Photoresponse mechanism of thin superconducting films and superconducting detectors", *Int. J. Mod. Phys.*, B 10, 1996.
- [8] K. Il'in, M. Lindgren, M. Currie, A. Semenov, G. Gol'tsman, R. Sobolewski, S. Cherednichenko, E. Gershenzon, "Picoscond hot-electron energy relaxation in NbN superconducting photodetectors", *Appl. Phys. Lett.*, vol. 76, 2000.
- [9] K. Ilin, R. Schneider, D. Gerthsen, A. Engel, H. Bartolf, A. Schilling, A. Semenov, H.-W. Huebers, B. Freitag and M. Siegel, "Ultra-thin NbN films on Si: crystalline and superconducting properties," *Journal of Physics: Conference Series*, vol. 97, p. 012045, 2008.
- [10] A. Kawakami, "Design and fabrication of NbN terahertz hot electron bolometer mixers," *24th Int. Symp. on Space Terahertz Technology*, 2013.
- [11] D. Dochev, V. Desmaris, A. Pavolotsky, D. Meledin, Z. Lai, A. Henry, E. Janzen, E. Pippel, J. Woltersdorf and V. Belitsky, "Growth and characterization of epitaxial ultra-thin NbN films on 3C-SiC/Si substrates for terahertz applications," *Supercond. Sci. Technol.*, 2011.
- [12] J. Gao, M. Hajenius, F. Tichelaar, T. Klapwijk, B. Voronov, "Monocrystalline NbN nanofilms on a 3C-SiC/Si substrate", *Appl. Phys. Lett.*, 2007.
- [13] S. Krause, D. Meledin, V. Desmaris, A. Pavolotsky, V. Belitsky, M. Rudzinski and E. Pippel, "Epitaxial growth of ultra-thin NbN films on AlxGa1-xN buffer-layers," *Supercond. Sci. Technol.*, vol. 27, no. 6, Apr 2014.
- [14] L. Kang, B. Jin, X. Liu, X. Jia and J. Chen, "Suppression of Superconductivity in epitaxial NbN ultrathin films," *Journal of Applied Physics*, vol. 109, 2011.
- [15] X. Q. Jia, L. Kang, M. Gu, X. Z. Yang, C. Chen, X. C. Tu, B. B. Jin, W. W. Xu, J. Chen and P. H. Wu, "Fabrication of a strain-induced high performance NbN ultra-thin film by a Nb5N6 buffer layer on Si substrate," *Supercond. Sc. Technol.*, vol. 27, p. 035010, 2014.
- [16] H. Ibach and D. L. Mills, *Electron Energy Loss Spectroscopy and Surface Vibrations*, New York: *Academic Press*, 1982.
- [17] R. Frankenthal, D. Siconolfi, W. Sinclair, D. Bacon, "Thermal Oxidation of Niobium Nitride Films at Temperatures from 20 °-400 °C", *J. Electrochem. Soc.: Solid-State Science and Technology*, vol. 130, no. 10 1983.
- [18] P. Gallagher, W. Sinclair, D. Bacon, G. Kammlott, "Oxidation of sputtered niobium nitride films", *J. Electrochem. Soc.: Solid-State Science and Technology*, vol. 130, no. 10 1983.
- [19] A. Ermolieff, M. Girard, C. Raoul, " An XPS comparative study on thermal oxide barrier formation on Nb and NbN thin films", *Applications of Surface Science*, vol. 21, p. 65, 1985.2 to
- [20] D. Bach, "EELS investigations of stoichiometric niobium oxides and niobium-based capacitors", Doctoral dissertation, Karlsruhe: Karlsruhe Insitute of Technology (KIT), 2009.
- [21] A. Stockhausen, *Optimization of Hot-Electron Bolometers for THz Radiation*, Karlsruhe: Karlsruhe Institute of Technology (KIT), KIT Scientific Publishing, 2013.
- [22] V. Afanas'ev, S. Krause, A. Lubenschenko, A. Batrakov, V. Desmaris, A. Pavolotsky, V. Belitsky, "Study of NbN ultra-thin films for THz hot-electron bolometers", *25th Int. Symp. on Space Terahertz Technology*, 2014.
- [23] S. Tanuma, C. J. Powell and D. R. Penn, "Calculations of electron inelastic mean free paths (IMFPs). IV. Evaluation of calculated IMFPs and of the predictive IMFP formula TPP-2 for electron energies between 50 and 2000 eV", *Surf. Interf. Anal.*, vol. 20, p. 77, 1993.
- [24] V. Afanas'ev, A. Lubenschenko, M. Lukashvsky, "Study of Al/Nb interface by spectroscopy of reflected electrons," *Journal of Applied Physics*, vol. 101, p. 064912, 2007.
- [25] S. Tougaard and I. Chorkendorff, "Differential inelastic electron scattering cross sections from experimental reflection electron-energy-loss spectra: Application to background removal in electron spectroscopy", *Phys. Rev. B*, vol. 35, p. 6570, 1987.